AMERICAN SOCIETY FOR MICROBIOLOGY | Infection and Immunity

Galectin-3 Plays an Important Role in Innate Immunity to Gastric Infection by *Helicobacter pylori*

Ah-Mee Park,[a] Satoru Hagiwara,[b] Daniel K. Hsu,[c] Fu-Tong Liu,[c] Osamu Yoshie[a]

Department of Microbiology[a] and Department of Gastroenterology and Hepatology,[b] Kindai University Faculty of Medicine, Osaka, Japan; Department of Dermatology, University of California Davis Health System, Sacramento, California, USA[c]

We studied the role of galectin-3 (Gal3) in gastric infection by *Helicobacter pylori*. We first demonstrated that Gal3 was selectively expressed by gastric surface epithelial cells and abundantly secreted into the surface mucus layer. We next inoculated *H. pylori* Sydney strain 1 into wild-type (WT) and Gal3-deficient mice using a stomach tube. At 2 weeks postinoculation, the bacterial cells were mostly trapped within the surface mucus layer in WT mice. In sharp contrast, they infiltrated deep into the gastric glands in Gal3-deficient mice. Bacterial loads in the gastric tissues were also much higher in Gal3-deficient mice than in WT mice. At 6 months postinoculation, *H. pylori* had successfully colonized within the gastric glands of both WT and Gal3-deficient mice, although the bacterial loads were still higher in the latter. Furthermore, large lymphoid clusters mostly consisting of B cells were frequently observed in the gastric submucosa of Gal3-deficient mice. *In vitro*, peritoneal macrophages from Gal3-deficient mice were inefficient in killing engulfed *H. pylori*. Furthermore, recombinant Gal3 not only induced rapid aggregation of *H. pylori* but also exerted a potent bactericidal effect on *H. pylori* as revealed by propidium iodide uptake and a morphological shift from spiral to coccoid form. However, a minor fraction of bacterial cells, probably transient phase variants of Gal3-binding sugar moieties, escaped killing by Gal3. Collectively, our data demonstrate that Gal3 plays an important role in innate immunity to infection and colonization of *H. pylori*.

Helicobacter pylori is a spiral-shaped, highly motile Gram-negative bacterium that selectively colonizes the human stomach. It infects about 50% of the world's population (1–3). Colonization of *H. pylori* in the gastric mucosa is etiologically associated with peptic ulcer and chronic gastritis. Furthermore, *H. pylori* colonization increases the risk of gastric adenocarcinoma and mucosa-associated lymphoid tissue (MALT) lymphoma (1–3). The virulence factors present in *H. pylori* strains contribute to gastric pathogenesis (1–3). However, overt gastric diseases are seen in only a fraction of infected hosts; the majority of colonized individuals remain mostly asymptomatic, while only 30% of those infected have gastric diseases of various severities (1–3). Thus, it is of interest to elucidate host factors that contribute to the control of gastric infection and colonization of *H. pylori*.

Adhesion to the gastric epithelium is known to be the first critical step for successful colonization of *H. pylori* (4). Previous studies have shown that surfactant protein D (SP-D) and mucins function as effective mucosal barriers against *H. pylori* infection (5, 6). SP-D is a member of calcium-dependent C-type lectins and belongs to a subfamily whose members are termed collectins (collagen lectins) and preferentially bind to monosaccharide units of the mannose type (7). Although SP-D was originally identified as a component of surfactant in the lung, where it is mainly expressed by type II alveolar cells and Clara cells, it is also expressed at other mucosal sites (7). In the gastric mucosa, SP-D is present in the luminal surface and its level increases in *H. pylori*-associated gastritis (5). *In vitro*, SP-D binds to *H. pylori* mainly via lipopolysaccharide (LPS), inhibits its motility, and induces its aggregation (5). Mucins, a family of highly *O*-glycosylated glycoproteins, also provide mucosal surface barriers against infectious pathogens (6). In particular, there are two types of mucin layer in the human gastric mucosa: the surface mucins secreted by surface mucous cells and the gland mucins secreted by gland mucous cells (8). Importantly, the gland mucins, which are rich in *O*-glycans with terminal α1,4-linked *N*-acetylglucosamine residues, have been shown to be directly microbicidal for *H. pylori* (9). This may explain why *H. pylori* bacterial cells are rarely present in the deeper portions of the gastric mucosa (9).

Galectins compose an evolutionary conserved family of β-galactoside binding proteins with 15 members known in mammals to date (10–13). Each member contains at least one domain of about 130 amino acids designated the carbohydrate recognition domain (CRD), which is responsible for the binding to galactose-containing sugar moieties. In particular, galectin-3 (Gal3), a unique chimeric type with an N-terminal nonlectin domain connected to a CRD domain, is highly expressed by activated macrophages and also by various cells, including epithelial cells (10). Gal3 is produced as a monomer but undergoes multimerization through its proline- and glycine-rich N-terminal domain upon binding to glycoconjugate ligands (10). Gal3 is found intracellularly in the nucleus or cytoplasm and is also secreted by nonclassical pathways, thus being present on the cell surface and in the extracellular space (14). Previous studies have shown that Gal3 is important in immune cell functions (15). For example, Gal3 is involved in macrophage survival and phagocytosis (16–18). Of note, the phagocytosis-promoting functions of Gal3 appear to operate mostly

Received 15 October 2015 **Returned for modification** 10 December 2015
Accepted 2 February 2016

Accepted manuscript posted online 8 February 2016

Citation Park A-M, Hagiwara S, Hsu DK, Liu F-T, Yoshie O. 2016. Galectin-3 plays an important role in innate immunity to gastric infection by *Helicobacter pylori*. Infect Immun 84:1184–1193. doi:10.1128/IAI.01299-15.

Editor: S. R. Blanke

Address correspondence to Ah-Mee Park, ampk@med.kindai.ac.jp, or Osamu Yoshie, o.yoshie@med.kindai.ac.jp.

through intracellular mechanisms, with Gal3 being localized in phagocytic cups and phagosomes of macrophages containing phagocytosed erythrocytes (18) or in bacterium-containing phagosomes of *Mycobacterium*-infected macrophages (17). Furthermore, extracellular Gal3 promotes neutrophil functions such as survival, phagocytosis, and extravasation (19–21). Gal3 also binds to LPS from various bacterial species and may serve as a negative regulator of LPS-induced inflammation, protecting hosts from endotoxin shock (22). Gal3 is even directly bacteriostatic against *Streptococcus pneumoniae* (19) and cytocidal to *Candida albicans* species bearing β-1,2-linked oligomannans (23). Gal3 immunoreactivity was reported to be restricted to the outer layer of the gastric mucosa in the stomach (24). Furthermore, Gal3 was shown to bind to *H. pylori* via its *O*-antigen side chain of LPS (25). However, the role of Gal3 in gastric infection by *H. pylori* has not been addressed.

In the present study, we performed gastric infection by *H. pylori* Sydney strain 1 in wild-type (WT) and Gal3-deficient mice. While the bacterial cells were mostly trapped in the surface mucus layer in WT mice, they infiltrated deep into the gastric glands in Gal3-deficient mice. Furthermore, macrophages from Gal3-deficient mice were inefficient in intracellular killing of engulfed *H. pylori*. Moreover, recombinant Gal3 rapidly aggregated and directly killed *H. pylori* bacterial cells *in vitro*. Collectively, our present results demonstrate that Gal3 is an important host factor in innate immunity to gastric infection and colonization of *H. pylori*.

MATERIALS AND METHODS

Antibodies and reagents. The polyclonal antibodies used were as follows: anti-Gal3 (BioLegend, San Diego, CA), anti-F4/80 (abd Serotec, Kidlington, United Kingdom), anti-CD45R (eBioscience, San Diego, CA), anti-CD3 (Biocare Medical, Concord, CA), and anti-*H. pylori* (Thermo Fisher Scientific, Fremont, CA). Alexa Fluor 546-conjugated anti-mouse IgG (H+L) was purchased from Thermo Fisher Scientific. Recombinant human and mouse Gal3 was purchased from R&D Systems (Minneapolis, MN). All other reagents were purchased from Wako (Osaka, Japan).

Bacterial strains. *H. pylori* Sydney strain 1 was originally isolated by Lee et al. (26). The *Escherichia coli* HST 08 strain was obtained from TaKaRa (Shiga, Japan). *H. pylori* colonies were formed on brucella agar (Becton Dickinson, Sparks, MD) supplemented with 7% fetal bovine serum (FBS) by incubation for 3 days at 37°C under microaerobic conditions using Anaeropack Microaero (Mitsubishi Gas Chemical, Tokyo, Japan). A single colony was isolated and inoculated into brucella broth (Becton Dickinson) supplemented with 7% FBS and cultured with constant shaking at 150 rpm. Cell numbers in suspensions were determined by analysis of optical density at 550 nm, with an optical density value of 0.2 corresponding to about 10^8 cells/ml. *E. coli* bacteria were cultured in LB medium (Sigma-Aldrich, St. Louis, MO) at 37°C. Cell numbers were determined by analysis of optical density at 550 nm, with a value of 0.1 corresponding to about 10^8 cells/ml.

Mice. CD1 mice were purchased from Charles River Laboratories Japan (Yokohama, Japan). The generation of Gal3-deficient mice was described previously (16). After transportation to Japan, Gal3-deficient mice were backcrossed to CD1 mice for nine generations. Mice at the age of 6 weeks were used for the experiments. The animal experiments were approved by the Institutional Animal Care and Use Committee of Kindai University and performed in accordance with the institutional guidelines.

Bacterial infection. Using a stomach tube, wild-type (WT) and Gal3-deficient mice were inoculated daily with 400 μl brucella broth containing 5×10^7 *H. pylori* bacteria for 5 days. Control mice were similarly inoculated with 400 μl brucella broth. At 2 weeks or 6 months after the last inoculation, mice were euthanized. After blood was taken from the left ventricle, the stomach was removed, washed in phosphate-buffered saline (PBS), and dissected longitudinally into three pieces. One piece was used for determination of bacterial load. Another piece was formalin fixed and embedded in paraffin for histological examinations. The last piece was stored at −80°C for later use. To perform quantitative culture, each gastric tissue was carefully weighed, placed in 1 ml of PBS, finely minced, and vigorously shaken for 10 min. After that, 10 μl of the supernatant was spread on brucella agar containing vancomycin (10 mg/liter), trimethoprim (5 mg/liter), amphotericin B (500 μg/liter), 5% FBS, and 2,3,5-triphenyltetrazolium chloride (50 mg/liter). Plates were kept at 37°C under microaerobic conditions for 4 days. Colonies were counted using Image J software (NIH, Bethesda, MD).

Immunological staining and PAS staining. Tissue sections of 4-μm thickness were made. Immunohistochemistry (IHC) was performed by the standard procedures using a Histofine SAB-PO kit (Nichirei Biosciences; Tokyo, Japan). Periodic acid-Schiff (PAS) staining was also performed by the standard procedures. For fluorescence staining, secondary antibodies labeled with Alexa 488 or Alexa 555 were used (Life Technologies, Carlsbad, CA). For nuclear staining, TO-PRO-3 (Life Technologies) was used. Fluorescent images were taken using a confocal laser microscope (Carl Zeiss GmBH, Jena, Germany).

Western blot analysis. Tissue homogenates were made in CelLytic MT (Sigma-Aldrich) containing Protease Inhibitor Cocktail Complete (Roche Diagnostics, Mannheim, Germany). Insoluble materials were removed by centrifugation. Gastric mucus was collected as reported previously (27). In brief, mice were anesthetized with pentobarbital. The abdominal wall and stomach were opened. After food particles were removed by the use of forceps, the pylorus was tied with sutures to avoid bile reflux. Gastric mucus was collected by vigorously pipetting 500 μl of 10 mM EDTA-HCl (pH 7.4). Particles were removed by brief centrifugation, and the remaining fluids were lyophilized. Lyophilized mucus fluids were dissolved with 100 μl CelLytic MT, pooled, and centrifuged. Tissue and mucus lysates were electrophoresed on an SDS-polyacrylamide gel under reducing conditions and electrophoretically transferred to a polyvinylidene fluoride (PVDF) membrane. Membranes were blocked with 5% skim milk and probed with primary antibodies. After washing was performed, membranes were reacted with horseradish peroxidase (HRP)-conjugated secondary antibodies and developed using an ECL Prime system (GE Healthcare, Piscataway, NJ).

Measurement of anti-*H. pylori* IgG. Serum anti-*H. pylori* IgG antibodies were measured using an enzyme-linked immunosorbent assay (ELISA) essentially as described previously (28). Briefly, 96-well MaxiSorp plates (Nunc, Kamstrup, Denmark) were coated with whole-cell lysates of *H. pylori* in carbonate-bicarbonate buffer (pH 9.5) containing 0.5% Triton X-100 at 25 μg protein per well. After washing and blocking with bovine serum albumin (BSA) were performed, 100-μl serum samples diluted at 1:100 were added to coated wells. After reactions were performed with HRP-conjugated goat anti-mouse IgG (Amersham, Les Ulis, France), plates were developed with a buffer containing 2,2′-azinobis(3-ethylbenzthiazoline-6-sulfonic acid) and hydrogen peroxide in citrate buffer (pH 4.0). After reactions were stopped with 10% SDS, the optical density at 405 nm was read on a microplate reader (Bio-Rad, Hercules, CA). Readings from uninfected control samples were subtracted as backgrounds.

Assays using peritoneal macrophages. Mice were kept unfed for 14 h, anesthetized with diethyl ether, bled from the carotid artery, and intraperitoneally injected with 3 ml PBS containing 2 mM EDTA twice to collect peritoneal lavage fluids. Cells in pooled lavage fluids were pelleted by centrifugation at 600 × *g* for 5 min and resuspended at 5×10^5/ml in RPMI 1640 (Life Technologies) supplemented with 10% FBS and antibiotics. Phagocytosis assays were performed as follows. Peritoneal cells were seeded in a 4-well glass plate at 2.5×10^5 cells/well and cultured at 37°C in 5% CO_2/95% air for 2 h. Floating cells were removed by washing, and adherent cells were further cultured for 1 h. Fluorescein isothiocyanate (FITC) beads (size, 2 μm) or *H. pylori* cells were added at 2.5×10^5

beads/well or 1.25×10^6 bacterial cells/well, respectively. After incubation for an indicated length of time, macrophages were washed, fixed with ice-cold ethanol, and stained with rhodamine-phalloidin (Thermo Fisher Scientific, Waltham, MA). *H. pylori* cells were stained with anti-*H. pylori* antibody. In some experiments, macrophages were stained with anti-Gal3 antibody. Nuclei were counterstained with TO-PRO-3. Fluorescent images were taken on a confocal laser microscope (Carl Zeiss). Cells containing FITC beads or *H. pylori* cells were analyzed using Image J software. Bacterial killing assays were performed as follows. Peritoneal cells were seeded in a 24-well plate at 2.5×10^5 cells/well and cultured at 37°C in 5% CO_2/95% air for 2 h. Floating cells were removed by washing, and adherent cells were further cultured for 1 h. *H. pylori* or *E. coli* bacteria were added at 1.25×10^6 cells/well or 2.5×10^4 cells/well, respectively. After incubation for 4 h at 37°C, macrophages were washed with PBS to remove free bacterial cells and lysed by treatment with 0.1% saponin for 15 min at 37°C. After brief centrifugation to remove cell debris, cell lysates were spread on agar plates. After an appropriate length of culture, bacterial colonies were counted (29, 30). Nitrite (NO_2^-) production assays were performed as follows. Peritoneal cells were seeded in a 24-well plate at 1.5×10^5 cells/well and cultured at 37°C in 5% CO_2/95% air for 2 h. Floating cells were removed by washing, and adherent cells were further cultured for 1 h. *H. pylori* bacteria were added at 7.5×10^5 cells/well in a total volume of 0.5 ml RPMI 1640 containing 10% FBS without phenol red. After incubation at 37°C in 5% CO_2/95% air for 48 h, culture supernatants were collected and cleared by centrifugation. Each sample (100 μl) was mixed with 100 μl of 1% Griess-Romijn nitrite reagent (Wako) (31). After incubation at room temperature for 10 min, the absorbance at 550 nm was read. Sodium nitrite was used as the standard.

Effect of recombinant Gal3 on *H. pylori*. *H. pylori* and *E. coli* were used in the mid-logarithmic growth phase. Bacterial cells were suspended in PBS (1×10^3 cells/10 μl), mixed with recombinant human Gal3, and incubated at 37°C in a 5% CO_2 incubator. In some experiments, lactose was added at 2 mM. After that, bacterial cells were pipetted and plated on agar and cultured at 37°C. Colonies were counted by Image J software. We also observed bacterial cells in the presence or absence of Gal3 on a glass slide using a microscope with a charge-coupled-device (CCD) camera (Olympus, Japan). Live and dead cells were differentiated by staining with carboxyfluorescein diacetate (CFDA) (Dojindo, Kumamoto, Japan) and propidium iodide (PI), respectively (32). Intracellular ATP contents were measured as follows. Bacterial cells in the mid-logarithmic growth phase were suspended in 50 mM HEPES (pH 7.4)-buffered saline and treated with various concentrations of recombinant Gal3 in the presence of 0.1 M sodium succinate at 37°C for 1 h. To extract ATP from cells, trichloroacetic acid (TCA) was added to give a final concentration of 1% and the solution was mixed well. Samples were neutralized with Tris-HCl (pH 8.0). ATP levels were measured using a chemiluminescent ATP assay kit (TOYO B-net, Tokyo, Japan) and a Wallac Arvo SX 1420 multilabel counter (PerkinElmer, Waltham, MA).

Scanning electron microscopic analysis. *H. pylori* and *E. coli* in mid-logarithmic growth phase were used. Bacterial cells were treated with 2.5 μM Gal3 for 1 h at 37°C in a 5% CO_2 incubator, fixed with 2.5% glutaraldehyde for 1 h, and immobilized to poly(L)-lysine-coated aluminum foil. After washing with 0.1 M phosphate buffer (pH 7.4) was performed, cells were treated with 1% osmium tetroxide for 2 h, rinsed twice with distilled water, and dehydrated with ethanol in a graded series. After treatment with isoamyl acetate, cells were dried with liquid carbon dioxide in a critical-point drying apparatus (HCP-1; Hitachi Koki, Tokyo, Japan), coated with 3-nm-thick platinum-palladium by evaporation in an E-1030 magnetron sputter coater (Hitachi, Ibaraki, Japan), and observed on an ultra-high-resolution scanning electron microscope (S-900; Hitachi) with an accelerating voltage of 10 kV.

Statistical analysis. Statistical analysis was performed using Student's *t* test. *P* values of <0.05 were considered significant.

RESULTS

Localization of Gal3 in the gastric mucosa. Using WT and Gal3-deficient mice, we first performed IHC of Gal3 in the whole gastrointestinal tract (Fig. 1A). The epithelial cells of the gastrointestinal tract generally expressed Gal3. In the case of gastric mucosa, however, the staining was mostly restricted to the surface epithelial cells as reported previously (24). We observed no gross abnormality in the gastric mucosa of Gal3-deficient mice by hematoxylin-eosin (HE) staining (not shown) or PAS staining (Fig. 1B). Immunoblot analysis demonstrated abundant Gal3 not only in the gastric tissue but also in the surface mucus layer (Fig. 1C). Thus, Gal3 is selectively expressed by surface epithelial cells of the gastric mucosa and abundantly secreted into the surface mucus layer. In our preliminary study, we also confirmed strong expression of Gal3 in the surface epithelial cells of human gastric tissues (data not shown).

***H. pylori* infection of WT and Gal3-deficient mice.** To examine the role of Gal3 in gastric infection by *H. pylori*, we inoculated 5×10^7 *H. pylori* cells into WT and Gal3-deficient mice daily for 5 days using a stomach tube. Two weeks after the last inoculation, we recovered bacterial cells from the stomach tissues and determined their numbers by colony formation on agar. As shown in Fig. 2A, the recovered bacterial cell numbers were about 4-fold higher in Gal3-deficient mice than in WT mice. The serum anti-*H. pylori* IgG titers were also about 3-fold higher in Gal3-deficient mice (Fig. 2B). These results suggested elevated levels of *H. pylori* infection in Gal3-deficient mice. We therefore performed IHC of *H. pylori* in gastric tissues of WT and Gal3-deficient mice (Fig. 2C). In the WT mice, the bacterial cells were mostly restricted to the surface mucus layer. In sharp contrast, the bacterial cells infiltrated deep within the gastric glands in the Gal3-deficient mice. We also performed double immunofluorescence staining of Gal3 (red) and *H. pylori* (green). As shown in Fig. 2D, the bacterial cells were mostly restricted to the surface mucus layer, colocalized with Gal3, and often aggregated in WT mice. On the other hand, the bacterial cells were found deep within the gastric glands in Gal3-deficient mice. Thus, in the presence of Gal3, *H. pylori* cells were mostly aggregated within the surface mucus layer and prevented from penetration into the deeper layers.

Long-term outcome of *H. pylori* infection. We also kept *H. pylori*-infected WT and Gal3-deficient mice until 6 months after the last inoculation. We noted reduced food consumption by *H. pylori*-infected Gal3-deficient mice that was probably due to loss of appetite. Accordingly, their average body weights at 6 months were significantly lower than those of *H. pylori*-infected WT mice and uninfected Gal3-deficient mice by 20% and 23%, respectively (Fig. 3A). This suggested some chronic gastric disease in *H. pylori*-infected Gal3-deficient mice. The bacterial recovery from stomach tissues was about 2-fold higher in Gal3-deficient mice than in WT mice (Fig. 3B). IHC of *H. pylori* in the gastric mucosa also demonstrated higher levels of bacterial cells in Gal3-deficient mice than in WT mice (Fig. 3C). Of note, however, bacterial cells now penetrated deep into the gastric glands even in WT mice. Thus, *H. pylori* had successfully colonized the gastric mucosa of WT mice at this time point. Upon microscopic inspection of the longitudinal gastric sections stained with HE, we also observed occasional lymphoid clusters in the gastric submucosa of the *H. pylori*-infected Gal3-deficient mice in particular. We confirmed that the majority of cells in such lymphoid clusters were $CD45R^+$ B cells, while

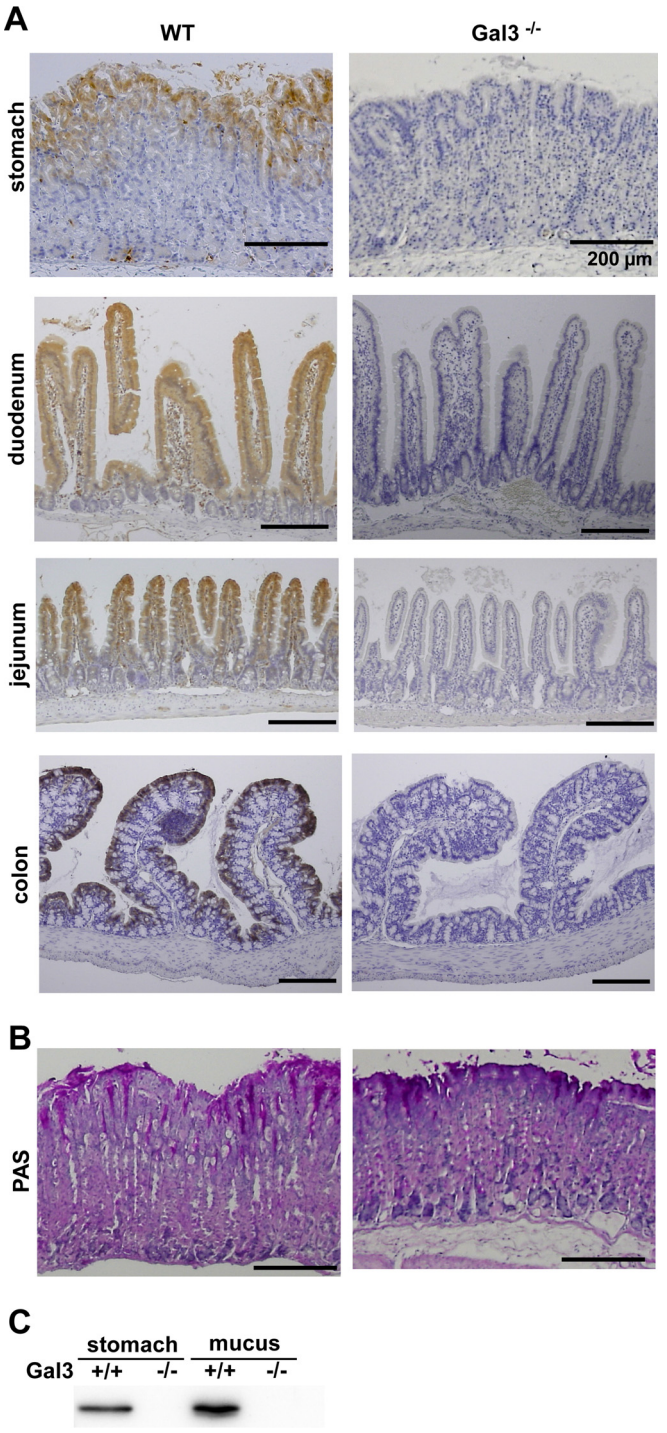

FIG 1 Localization of Gal3 in the mouse stomach. (A) Immunohistochemistry (IHC) for Gal3. IHC was performed for Gal3 using tissue sections from formalin-fixed and paraffin-embedded gastrointestinal tracts obtained from WT and Gal3-deficient mice. Representative results from four different anatomical locations are shown ($n = 7$). (B) PAS staining. Tissue sections from formalin-fixed and paraffin-embedded gastric tissues were stained with PAS. Representative results are shown ($n = 7$). (C) Immunoblot analysis for Gal3. Lysates were prepared from gastric tissues and surface mucus layer samples obtained from WT and Gal3-deficient mice. Immunoblot analysis was performed for Gal3. Representative results from three separate experiments are shown.

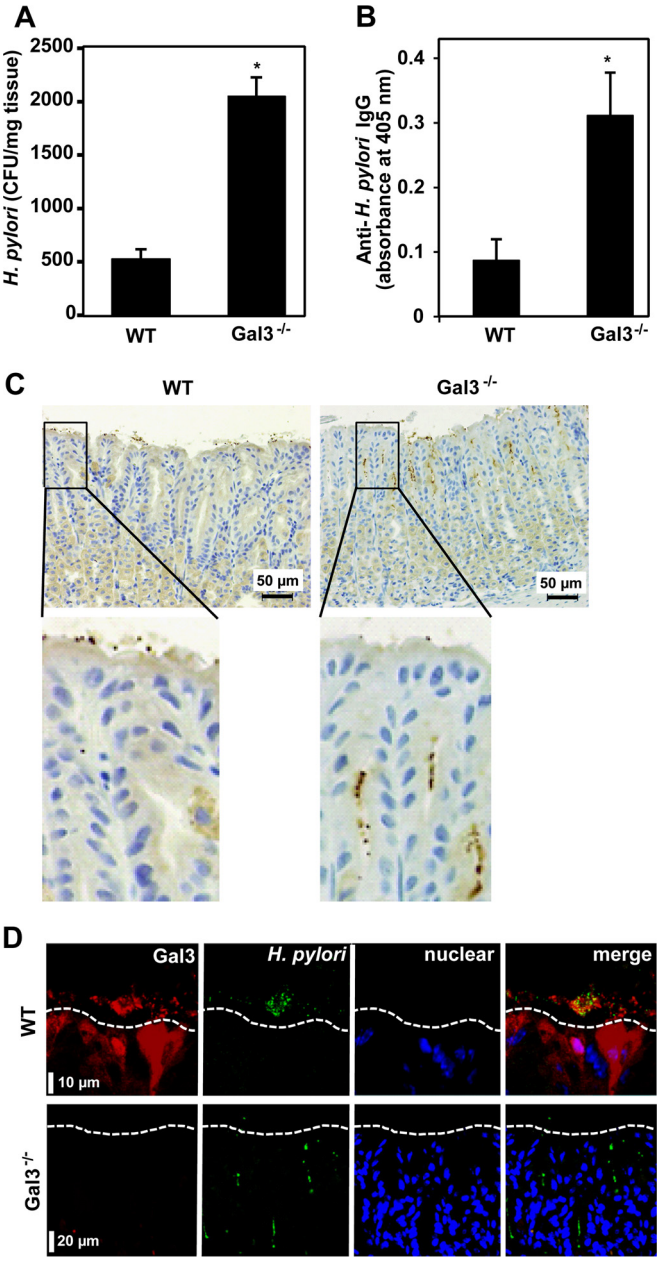

FIG 2 Role of Gal3 in *H. pylori* infection. WT and Gal3-deficient mice were inoculated with 5×10^7 *H. pylori* cells daily for 5 days using a stomach tube. Two weeks after the last inoculation, mice were sacrificed and samples were taken. (A) Quantitation of *H. pylori* cells in the stomach. After washing in PBS was performed, excised stomach tissues were finely minced and vigorously shaken in PBS for 10 min. Supernatants were plated on brucella agar plates and cultured at 37°C for 4 days under microaerobic conditions. Colonies were counted by using Image J software. Data are shown as means ± standard deviations (SD) ($n = 7$). *, $P < 0.05$. (B) Measurement of serum anti-*H. pylori* IgG levels. An ELISA was used to determine serum anti-*H. pylori* IgG contents. Data are shown as means ± SD ($n = 7$). *, $P < 0.05$. (C) IHC of *H. pylori*. The bacterial cells were stained by IHC in formalin-fixed and paraffin-embedded gastric tissue sections (brown dots). Nuclei were counterstained with hematoxylin (blue). Magnified images of the squared regions are shown below. Representative results from three separate experiments are shown. (D) Immunofluorescence staining of Gal3 and *H. pylori*. Tissue sections were stained for Gal3 (red) and *H. pylori* (green) using secondary antibodies conjugated with Alexa 555 and Alexa 488, respectively. Nuclear DNA was counterstained with TO-PRO-3 (blue). The white dotted lines indicate the mucosal surface of the stomach. Representative results from four separate experiments are shown.

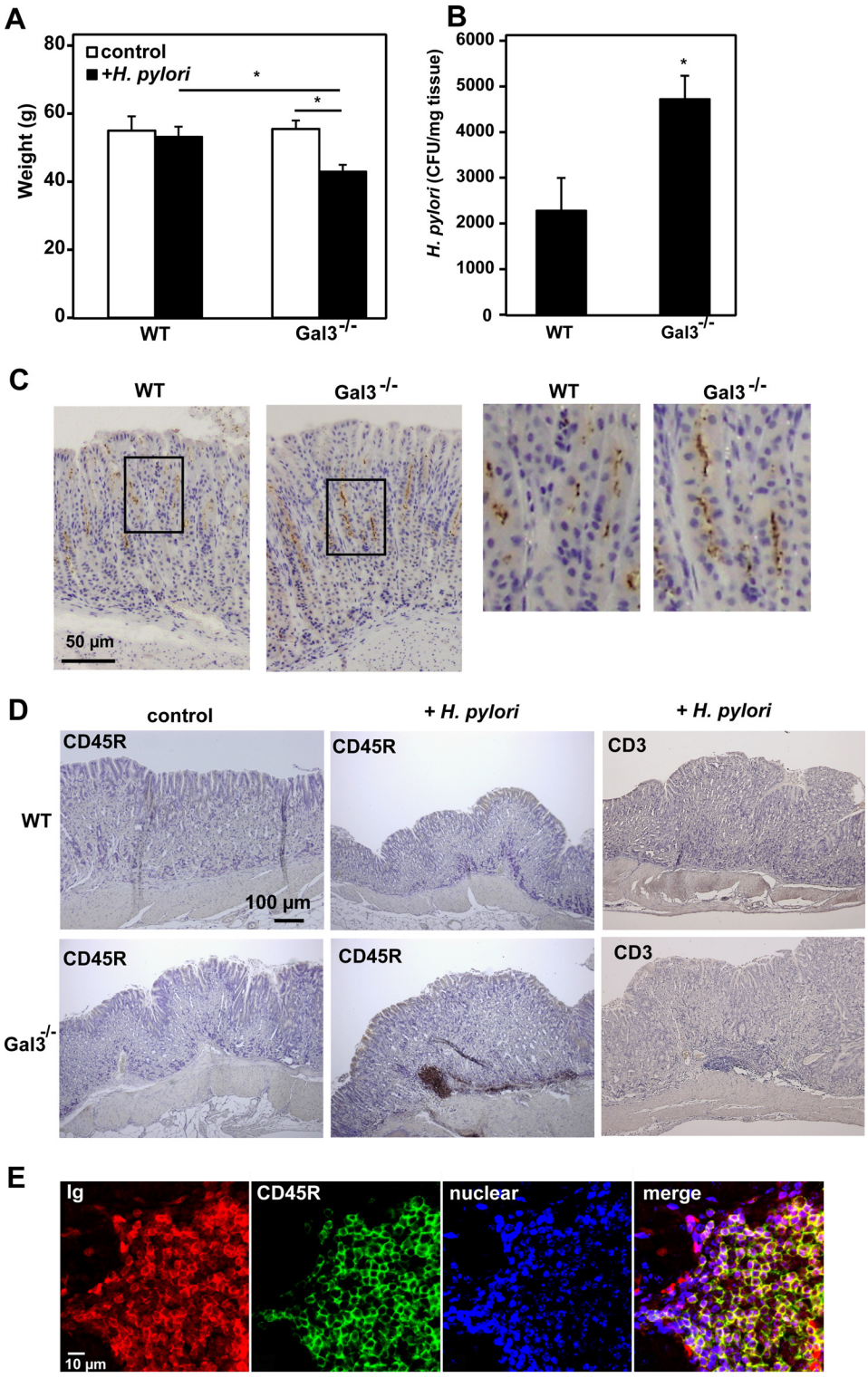

FIG 3 Long-term outcome of *H. pylori* infection. WT and Gal3-deficient mice were inoculated with 5×10^7 *H. pylori* cells daily for 5 days using a stomach tube. Six months after the last inoculation, body weights were measured and samples were taken. (A) Average body weights. Data are shown as means ± standard errors (SE) ($n = 8$). *, $P < 0.05$. (B) Quantitation of *H. pylori* cells. After washing in PBS was performed, excised gastric tissues were finely minced and vigorously shaken in PBS for 10 min. Supernatants were plated on brucella agar plates and cultured at 37°C for 4 days under microaerobic conditions. Formed colonies were counted using Image J software. Data are shown as means ± SE ($n = 8$). *, $P < 0.05$. (C) IHC of *H. pylori*. Formalin-fixed and paraffin-embedded gastric tissue sections were immunohistochemically stained for *H. pylori* (brown dots). Nuclei were counterstained with hematoxylin (blue). Magnified images of the squared regions are shown on the right. Representative results are shown ($n = 8$). (D) IHC of gastric tissue. IHC was performed for CD45R and CD3 using formalin-fixed and paraffin-embedded gastric tissue sections. Representative results are shown ($n = 8$). (E) Immunofluorescent staining of gastric tissue. Double immunofluorescent staining was performed for IgG (H+L) (red) and CD45R (green). Nuclei were counterstained with TO-PRO-3 (blue). Representative results are shown ($n = 6$).

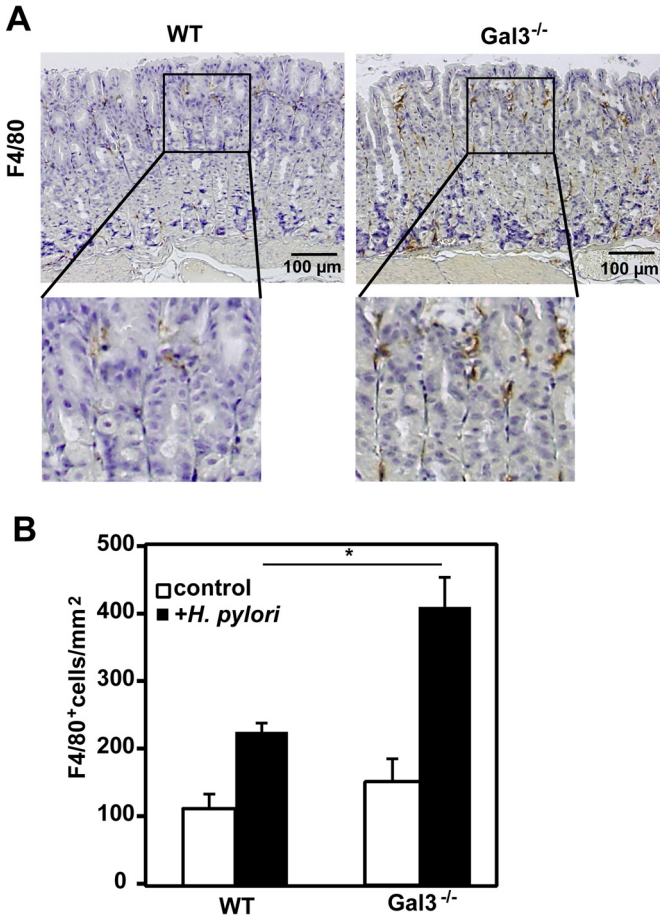

FIG 4 Tissue infiltration of macrophages. WT and Gal3-deficient mice were inoculated with 5×10^7 *H. pylori* cells daily for 5 days using a stomach tube. Two weeks after the last inoculation, mice were sacrificed and samples were taken. (A) Detection of macrophages. IHC was performed using formalin-fixed and paraffin-embedded gastric tissue sections. Macrophages were detected as F4/80$^+$ cells. Magnified images of the squared regions are shown below. Representative results are shown ($n = 7$). (B) Enumeration of macrophages. F4/80$^+$ cells were counted using Image J software. Data are shown as means ± SE ($n = 7$). *, $P < 0.05$.

CD3$^+$ T cells were scarce (Fig. 3D). The lymphoid cells were also strongly stained by anti-mouse IgG (H+L), further confirming that these cells were Ig-positive B cells (Fig. 3E). Since we were unable to detect lymphoid clusters by macroscopic inspection of the gastric tissues, we microscopically examined a single longitudinal gastric section from each mouse. While we observed no such lymphoid clusters in the sections from uninfected WT and Gal3-deficient mice ($n = 5$ each), we found a relatively large (>50-μm) lymphoid cluster in 1 of 8 WT mice and 5 of 8 Gal3-deficient mice ($P < 0.05$). Thus, a long-term colonization of *H. pylori* appeared to promote formation of lymphoid clusters, predominantly consisting of B cells, especially in Gal3-deficient mice.

Defective killing of *H. pylori* by Gal3-deficient macrophages. We next examined host cellular responses to *H. pylori* infection at 2 weeks after the last inoculation. As shown in Fig. 4A, F4/80$^+$ macrophages were the predominant infiltrating cells in the gastric mucosa of *H. pylori*-infected mice and their numbers were much higher in Gal3-deficient mice than in WT mice (Fig. 4B). On the other hand, we hardly observed any significant infiltration of neutrophils, B cells, or T cells in *H. pylori*-infected gastric mucosa at this time point (data not shown). Acute cellular responses in the gastric mucosa were also reported to be quite mild in human cases of *H. pylori* infection (33, 34).

Given that Gal3 is known to be abundantly expressed by macrophages (10), we next examined the effect of Gal3 deficiency on macrophage functions. Comparing peritoneal macrophages from WT and Gal3-deficient mice, we observed no significant differences in the uptake of FITC beads or *H. pylori* bacterial cells (Fig. 5A). However, macrophages from Gal3-deficient mice were less efficient in killing of engulfed *H. pylori* as revealed by much higher recovery of live bacterial cells from macrophage cell lysates (Fig. 5B). For comparison, we also performed the same experiments using *E. coli* as another species of Gram-negative intestinal bacteria. No differences between WT and Gal3-deficient macrophages in the recovery of *E. coli* were seen (Fig. 5B). Furthermore, no differences between WT and Gal3-deficient macrophages in nitric oxide production were seen upon incubation with *H. pylori* (Fig. 5C). By double immunofluorescence staining, we observed frequent colocalization of *H. pylori* (red) and Gal3 (green) within WT macrophages (Fig. 5D). This suggested direct interactions between Gal3 and ingested *H. pylori* bacterial cells within macrophages.

Effect of Gal3 on *H. pylori*. We next examined the direct effect of Gal3 on *H. pylori*. For comparison, *E. coli* was also tested. *H. pylori* and *E. coli* bacteria were treated with recombinant human Gal3 for 1 h. After vigorous pipetting was performed, bacterial cells were spread on agar plates and cultured to determine CFU. As shown in Fig. 6A, Gal3 dose dependently reduced CFU of *H. pylori* but not those of *E. coli*. We confirmed that lactose used as a competitive inhibitor abrogated the effect of Gal3 (Fig. 6B). Similar results were obtained by using recombinant mouse Gal3 (data not shown). Under the microscope, we observed that highly motile *H. pylori* bacterial cells quickly aggregated in the presence of Gal3 (Fig. 6C), most probably because of the multimer formation of Gal3 upon binding to *H. pylori* (10). This was also consistent with the *in vivo* observation that *H. pylori* bacterial cells often aggregated within the gastric surface mucus layer of WT mice (Fig. 2D). On the other hand, Gal3 induced no such aggregations in *E. coli* (Fig. 6C). However, the aggregation *per se* might not be the main cause of reduction in CFU of *H. pylori* by Gal3. This was because the colony sizes or required incubation times were not appreciably different between control and Gal3-treated *H. pylori* bacteria. We therefore stained Gal3-treated *H. pylori* bacterial cells with CFDA (green [live cells]) and PI (red [dead cells]). As shown in Fig. 6D, while the untreated bacterial cells that were stained with CFDA were mostly live cells, the majority of Gal3-treated bacterial cells were considered dead, as revealed by staining with PI. Lactose again prevented the bactericidal effect of Gal3. *H. pylori* bacteria are also known to change shape from spiral to coccoid under unfavorable conditions (35). As shown in Fig. 6E, scanning electron microscopy revealed that the majority of Gal3-treated *H. pylori* bacterial cells showed coccoid forms with numerous surface blebs, while Gal3 had no such effect on *E. coli*. Since the measurement of cellular ATP content is frequently used to determine live bacterial cell numbers, we also determined ATP contents in control and Gal3-treated bacterial cultures. Unexpectedly, Gal3 dose dependently increased cellular ATP contents in *H. pylori* within 1 h (Fig. 6F). No such effect was seen in *E. coli*. Taking the results together, Gal3 directly exerts a potent antimicrobial effect on *H. pylori*.

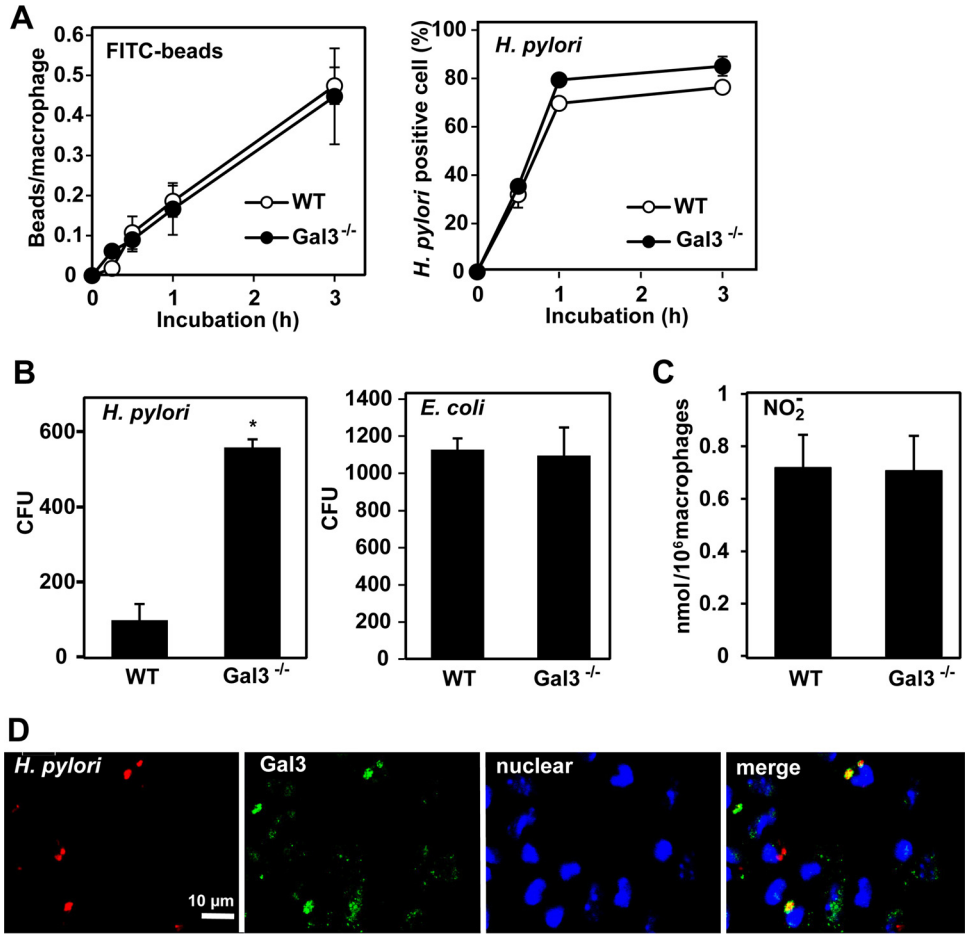

FIG 5 Role of Gal3 in macrophage function. Peritoneal macrophages were obtained from WT and Gal3-deficient mice. (A) Phagocytosis assay. Macrophages were incubated with FITC beads (2 μm) or *H. pylori* cells at 37°C. At the indicated time points, macrophages were fixed. For detection of FITC beads (green), fixed macrophages were stained with TO-PRO-3 for nuclei (blue) and with rhodamine-phalloidin for cytoskeleton (red). For detection of intracellular *H. pylori*, fixed macrophages were first stained for *H. pylori* (green) and then stained with TO-PRO-3 for nuclei (blue) and with rhodamine-phalloidin for cytoskeleton (red). Cells containing FITC beads or *H. pylori* were counted using Image J software. Data are shown as means ± SE ($n = 5$). (B) Intracellular killing assay. Macrophages were incubated with *H. pylori* or *E. coli* at 37°C for 4 h. After washing with PBS was performed, cell lysates were prepared with 0.1% saponin, spread on agar plates, and cultured at 37°C. Colonies were counted using Image J software. Data are shown as means ± SE ($n = 6$). *, $P < 0.05$. (C) NO_2^- production assay. Macrophages were incubated with *H. pylori* at 37°C for 2 days. Culture supernatants were collected and mixed with 1% Griess-Romijn nitrite reagent. Absorbance at 550 nm was read. Data are shown as means ± SE ($n = 6$). (D) Immunofluorescence staining. Macrophages were incubated with *H. pylori* at 37°C for 30 min. After washing was performed, macrophages were fixed and stained for *H. pylori* (red) and Gal3 (green). Nuclei were counterstained with TO-PRO-3 (blue). Fluorescent images were taken on a confocal laser microscope. Representative results from four separate experiments are shown.

Existence of *H. pylori* phase variants evading Gal3. Using the microscope, we also noticed a minor fraction of *H. pylori* bacterial cells that were freely moving and PI negative even in the presence of high concentrations of Gal3. We therefore isolated individual colonies formed by Gal3-treated *H. pylori*, expanded the colonies, and treated again with 2 μM Gal3. As shown in Fig. 6G, Gal3 again effectively reduced colony formation by each clone ($n = 5$). The results suggested that the minor fraction of *H. pylori* bacterial cells unaffected by high concentrations of Gal3 were not genetic mutants but were transient phase variants in terms of Gal3-binding sugar moieties.

DISCUSSION

Previously, Fowler et al. reported that Gal3 was able to bind to *H. pylori* via *O*-antigen side chains of LPS (25). Furthermore, the authors demonstrated that Gal3 was rapidly upregulated and secreted by a human gastric epithelial AGS cell line upon interaction with *H. pylori* (25). Gal3 was also reported to function as the gastric receptor for polymeric Lewis (X) on *H. pylori* cells, which express Lewis and related antigens along the *O*-antigen side chains (36). However, the role of Gal3 in gastric infection and colonization of *H. pylori* has not been addressed. In the present study, we showed that Gal3 provides an effective physical and biological barrier against gastric infection by *H. pylori*. As previously reported (24), Gal3 is selectively expressed by the surface epithelial cells of the gastric mucosa and abundantly secreted into the surface mucus (Fig. 1). In the presence of Gal3, *H. pylori* bacteria were mostly trapped within the surface mucus layer where the bacterial cells were also mostly aggregated (Fig. 2). Without Gal3, however, *H. pylori* easily migrated deep into the gastric glands (Fig. 2). Given that gastric colonization of *H. pylori* requires adhesion to epithelial cells (4), trapping and aggregation of bacterial cells

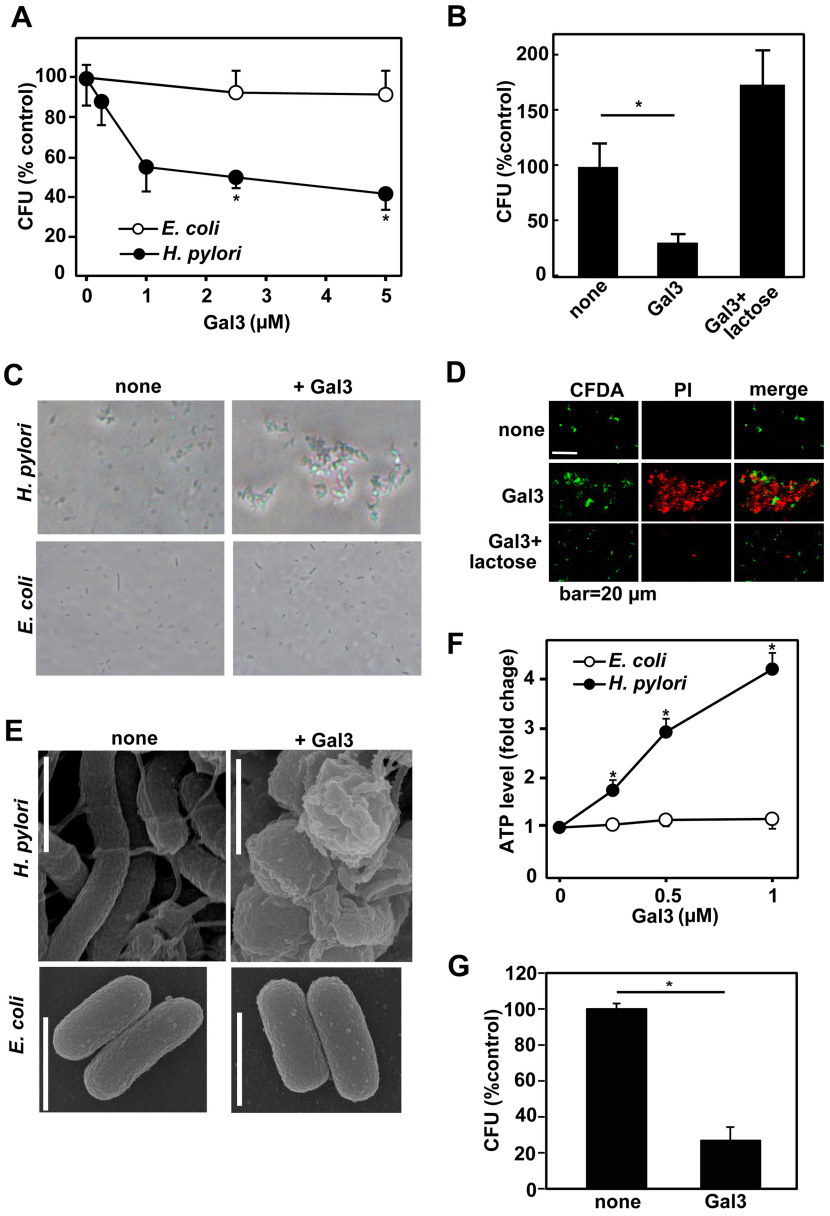

FIG 6 Effect of recombinant Gal3 on *H. pylori*. *H. pylori* and *E. coli* in the mid-logarithmic growth phase were used. Bacterial cells were suspended in PBS (1×10^3 cells/10 μl), mixed with recombinant human Gal3, and incubated at 37°C in a 5% CO_2 incubator. (A) Colony-forming assay. *H. pylori* and *E. coli* bacteria were suspended in PBS and treated with indicated concentrations of recombinant human Gal3 at 37°C for 1 h. Viable bacteria were quantitated by colony formation on agar. Data are shown as means ± SD ($n = 6$). *, $P < 0.05$. (B) Effect of lactose. *H. pylori* bacteria were incubated with 2 μM Gal3 with or without 2 mM lactose at 37°C for 1 h. Viable bacteria were quantitated by colony formation on agar. Data are shown as means ± SD ($n = 6$). *, $P < 0.05$. (C) Microscopic observation. *H. pylori* and *E. coli* bacteria were suspended in PBS and treated with 2.5 μM Gal3 for 10 min. Microscopic images were taken. Representative results from six separate experiments are shown. (D) Bactericidal assay. *H. pylori* cells were suspended in PBS and treated with 2 μM Gal3 without or with 2 mM lactose for 10 min in the presence of CFDA (the live-bacterium staining reagent) (green). After incubation, killed cells were stained with PI (red). Representative results from four separate experiments are shown. (E) Scanning electron microscopic observation. *H. pylori* and *E. coli* bacteria were suspended in PBS and treated with 2.5 μM Gal3 for 1 h. Images were taken on a scanning electron microscope. Bar, 1 μm. Representative results from three separate experiments are shown. (F) Measurement of cellular ATP content. *H. pylori* and *E. coli* bacteria were suspended in HEPES-buffered saline (pH 7.4) and treated with indicated concentrations of Gal3 at 37°C for 1 h. Cellular ATP contents were determined by using luciferase-catalyzed luciferin chemiluminescence. Data are shown as means ± SD ($n = 3$). *, $P < 0.05$. (G) Analysis of Gal3-resistant clones. *H. pylori* bacteria were incubated with 2 μM Gal3 at 37°C for 1 h and spread on agar plates. Formed colonies were individually isolated and expanded in liquid culture. The expanded clones were then treated with 2 μM Gal3 at 37°C for 1 h. Viable bacteria were quantitated by colony formation on agar. Data are shown as means ± SD ($n = 5$). *, $P < 0.05$.

within the surface mucus layer by Gal3 could be important host protective mechanisms against *H. pylori* infection and colonization. This would also promote clearance of *H. pylori* bacterial cells from the gastric mucosa by ciliary movement. Of note, *H. pylori* bacterial cells were also frequently found in small aggregates within the surface mucous layer and rarely present in deeper portions of the human gastric mucosa (37). We also demonstrated that Gal3-deficient macrophages were inefficient in killing of en-

gulfed *H. pylori* (Fig. 5). We have further demonstrated that recombinant Gal3 rapidly induces aggregation of *H. pylori*, most probably because of the multimerization of Gal3 upon binding to glycoconjugate ligands (10), and also exerts a potent bactericidal effect on *H. pylori* (Fig. 6). We speculate that this direct bactericidal activity of Gal3 against *H. pylori* could partly relate to the inefficient killing of engulfed *H. pylori* by Gal3-deficient macrophages (Fig. 5). On the other hand, Gal3 did not induce aggregation or killing of *E. coli* (Fig. 6). This is most likely due to its inability to bind to LPS of the *E. coli* strain used. Given that Gal3 is strongly expressed by epithelial cells of the colon (Fig. 1), *E. coli* may have evolved to evade recognition by Gal3. At present, we do not know the exact mechanism of *H. pylori* killing by Gal3, but we observed paradoxical sharp increases of the cellular ATP content in Gal3-treated *H. pylori* (Fig. 6), suggesting strong metabolic disturbances. In fact, previous studies have also described similar increases in cellular ATP content in stressed *H. pylori* (38, 39).

The bactericidal effect of Gal3 against *H. pylori* was incomplete (Fig. 6). Similar incomplete killing was also observed in Gal3-treated *C. albicans* (23). In this context, we observed that a minor fraction of *H. pylori* bacterial cells were not aggregated or killed even by high concentrations of Gal3. Furthermore, when we expanded colonies formed by Gal3-treated *H. pylori* and treated each clone with Gal3 again, they were again highly susceptible to Gal3, being rapidly aggregated and killed (Fig. 6). This indicated that the minor fraction of *H. pylori* bacterial cells resistant to Gal3 consisted not of mutants but of phase variants in terms of Gal3-binding sugar moieties. Thus, some differences in glycosylation patterns or densities on the surface allow a fraction of *H. pylori* cells to evade the bactericidal activity of Gal3. Of note, Khamri et al. also demonstrated that *H. pylori* could evade the binding of SP-D through phase variations in fucosylation of the *O*-antigen side chains of LPS (40).

We observed successful colonization of *H. pylori* in the gastric mucosa of not only Gal3-deficient mice but also WT mice at 6 months postinfection (Fig. 3). As mentioned above, the existence of transient phase variants in terms of Gal3-binding sugar moieties may account for the eventual success of *H. pylori* in penetration of the surface mucus layer and colonization within the deep layer of gastric glands where the production of Gal3 is low (Fig. 1). Nevertheless, Gal3 may still play an important role in host control of *H. pylori* colonization since *H. pylori*-infected Gal3-deficient mice showed higher recovery of bacterial cells and also significant reduction in average body weight compared to *H. pylori*-infected WT mice (Fig. 3). Furthermore, we observed formation of submucosal lymphoid clusters predominantly consisting of B cells, especially in Gal3-deficient mice (Fig. 3). This may be related to the pathogenesis of MALT lymphoma in humans by chronic *H. pylori* colonization (41). The results may also be remarkable in that a previous study observed no MALT lymphoma formation in WT mice infected with *H. pylori* Sydney strain 1 even after the 2-year follow-up period (42). Thus, Gal3-deficient mice may provide a useful model for the study of MALT lymphomagenesis by colonization with *H. pylori* Sydney strain 1 (43, 44).

In conclusion, we have demonstrated that Gal3 provides an effective physical and biological barrier against gastric infection by *H. pylori*. Gal3 not only efficiently traps and aggregates *H. pylori* within the gastric surface mucus layer but also exerts a potent bactericidal activity both directly and within macrophages. Thus, Gal3 could be an important host factor in keeping *H. pylori* infection and colonization at subclinical levels.

ACKNOWLEDGMENTS

We thank Yasumitsu Akahoshi and Yoshitaka Horiuchi for their excellent technical support.

This work was partly supported by MEXT KAKENHI grant 15K08975 to Ah-Mee Park.

FUNDING INFORMATION

MEXT KAKENHI provided funding to Ah-Mee Park under grant number 15K08975.

REFERENCES

1. **Atherton JC.** 2006. The pathogenesis of *Helicobacter pylori*-induced gastro-duodenal diseases. Annu Rev Pathol **1:**63–96. http://dx.doi.org/10.1146/annurev.pathol.1.110304.100125.
2. **Salama NR, Hartung ML, Muller A.** 2013. Life in the human stomach: persistence strategies of the bacterial pathogen *Helicobacter pylori*. Nat Rev Microbiol **11:**385–399. http://dx.doi.org/10.1038/nrmicro3016.
3. **Pereira MI, Medeiros JA.** 2014. Role of *Helicobacter pylori* in gastric mucosa-associated lymphoid tissue lymphomas. World J Gastroenterol **20:**684–698. http://dx.doi.org/10.3748/wjg.v20.i3.684.
4. **Guruge JL, Falk PG, Lorenz RG, Dans M, Wirth HP, Blaser MJ, Berg DE, Gordon JI.** 1998. Epithelial attachment alters the outcome of *Helicobacter pylori* infection. Proc Natl Acad Sci U S A **95:**3925–3930. http://dx.doi.org/10.1073/pnas.95.7.3925.
5. **Murray E, Khamri W, Walker MM, Eggleton P, Moran AP, Ferris JA, Knapp S, Karim QN, Worku M, Strong P, Reid KB, Thursz MR.** 2002. Expression of surfactant protein D in the human gastric mucosa and during *Helicobacter pylori* infection. Infect Immun **70:**1481–1487. http://dx.doi.org/10.1128/IAI.70.3.1481-1487.2002.
6. **Corfield AP.** 2015. Mucins: a biologically relevant glycan barrier in mucosal protection. Biochim Biophys Acta **1850:**236–252. http://dx.doi.org/10.1016/j.bbagen.2014.05.003.
7. **van de Wetering JK, van Golde LM, Batenburg JJ.** 2004. Collectins: players of the innate immune system. Eur J Biochem **271:**1229–1249. http://dx.doi.org/10.1111/j.1432-1033.2004.04040.x.
8. **Ota H, Katsuyama T, Ishii K, Nakayama J, Shiozawa T, Tsukahara Y.** 1991. A dual staining method for identifying mucins of different gastric epithelial mucous cells. Histochem J **23:**22–28. http://dx.doi.org/10.1007/BF01886504.
9. **Kawakubo M, Ito Y, Okimura Y, Kobayashi M, Sakura K, Kasama S, Fukuda MN, Fukuda M, Katsuyama T, Nakayama J.** 2004. Natural antibiotic function of a human gastric mucin against *Helicobacter pylori* infection. Science **305:**1003–1006. http://dx.doi.org/10.1126/science.1099250.
10. **Barondes SH, Cooper DN, Gitt MA, Leffler H.** 1994. Galectins. Structure and function of a large family of animal lectins. J Biol Chem **269:**20807–20810.
11. **Barondes SH, Castronovo V, Cooper DN, Cummings RD, Drickamer K, Feizi T, Gitt MA, Hirabayashi J, Hughes C, Kasai K, Leffler H, Liu FT, Lotan R, Mercurio AM, Monsigny M, Pillai S, Poirer F, Raz A, Rigby PWJ, Rini JM, Wang JL.** 1994. Galectins: a family of animal beta-galactoside-binding lectins. Cell **76:**597–598. http://dx.doi.org/10.1016/0092-8674(94)90498-7.
12. **Rabinovich GA, Baum LG, Tinari N, Paganelli R, Natoli C, Liu FT, Iacobelli S.** 2002. Galectins and their ligands: amplifiers, silencers or tuners of the inflammatory response? Trends Immunol **23:**313–320. http://dx.doi.org/10.1016/S1471-4906(02)02232-9.
13. **Vasta GR.** 2009. Roles of galectins in infection. Nat Rev Microbiol **7:**424–438. http://dx.doi.org/10.1038/nrmicro2146.
14. **Dumic J, Dabelic S, Flogel M.** 2006. Galectin-3: an open-ended story. Biochim Biophys Acta **1760:**616–635. http://dx.doi.org/10.1016/j.bbagen.2005.12.020.
15. **Sato S, Nieminen J.** 2004. Seeing strangers or announcing "danger": galectin-3 in two models of innate immunity. Glycoconj J **19:**583–591.
16. **Hsu DK, Yang RY, Pan Z, Yu L, Salomon DR, Fung-Leung WP, Liu FT.** 2000. Targeted disruption of the galectin-3 gene results in attenuated peritoneal inflammatory responses. Am J Pathol **156:**1073–1083. http://dx.doi.org/10.1016/S0002-9440(10)64975-9.
17. **Beatty WL, Rhoades ER, Hsu DK, Liu FT, Russell DG.** 2002. Association

of a macrophage galactoside-binding protein with *Mycobacterium*-containing phagosomes. Cell Microbiol **4:**167–176. http://dx.doi.org/10.1046/j.1462-5822.2002.00183.x.

18. **Sano H, Hsu DK, Apgar JR, Yu L, Sharma BB, Kuwabara I, Izui S, Liu FT.** 2003. Critical role of galectin-3 in phagocytosis by macrophages. J Clin Invest **112:**389–397. http://dx.doi.org/10.1172/JCI200317592.
19. **Farnworth SL, Henderson NC, Mackinnon AC, Atkinson KM, Wilkinson T, Dhaliwal K, Hayashi K, Simpson AJ, Rossi AG, Haslett C, Sethi T.** 2008. Galectin-3 reduces the severity of pneumococcal pneumonia by augmenting neutrophil function. Am J Pathol **172:**395–405. http://dx.doi.org/10.2353/ajpath.2008.070870.
20. **Sato S, Ouellet N, Pelletier I, Simard M, Rancourt A, Bergeron MG.** 2002. Role of galectin-3 as an adhesion molecule for neutrophil extravasation during streptococcal pneumonia. J Immunol **168:**1813–1822. http://dx.doi.org/10.4049/jimmunol.168.4.1813.
21. **Fermino ML, Polli CD, Toledo KA, Liu FT, Hsu DK, Roque-Barreira MC, Pereira-da-Silva G, Bernardes ES, Halbwachs-Mecarelli L.** 2011. LPS-induced galectin-3 oligomerization results in enhancement of neutrophil activation. PLoS One **6:**e26004. http://dx.doi.org/10.1371/journal.pone.0026004.
22. **Li Y, Komai-Koma M, Gilchrist DS, Hsu DK, Liu FT, Springall T, Xu D.** 2008. Galectin-3 is a negative regulator of lipopolysaccharide-mediated inflammation. J Immunol **181:**2781–2789. http://dx.doi.org/10.4049/jimmunol.181.4.2781.
23. **Kohatsu L, Hsu DK, Jegalian AG, Liu FT, Baum LG.** 2006. Galectin-3 induces death of *Candida* species expressing specific beta-1,2-linked mannans. J Immunol **177:**4718–4726. http://dx.doi.org/10.4049/jimmunol.177.7.4718.
24. **Nio-Kobayashi J, Takahashi-Iwanaga H, Iwanaga T.** 2009. Immunohistochemical localization of six galectin subtypes in the mouse digestive tract. J Histochem Cytochem **57:**41–50.
25. **Fowler M, Thomas RJ, Atherton J, Roberts IS, High NJ.** 2006. Galectin-3 binds to *Helicobacter pylori O*-antigen: it is upregulated and rapidly secreted by gastric epithelial cells in response to *H. pylori* adhesion. Cell Microbiol **8:**44–54. http://dx.doi.org/10.1111/j.1462-5822.2005.00599.x.
26. **Lee A, O'Rourke J, De Ungria MC, Robertson B, Daskalopoulos G, Dixon MF.** 1997. A standardized mouse model of Helicobacter pylori infection: introducing the Sydney strain. Gastroenterology **112:**1386–1397. http://dx.doi.org/10.1016/S0016-5085(97)70155-0.
27. **Bagshaw PF, Munster DJ, Wilson JG.** 1987. Molecular weight of gastric mucus glycoprotein is a determinant of the degree of subsequent aspirin induced chronic gastric ulceration in the rat. Gut **28:**287–293. http://dx.doi.org/10.1136/gut.28.3.287.
28. **Nagata K, Mizuta T, Tonokatu Y, Fukuda Y, Okamura H, Hayashi T, Shimoyama T, Tamura T.** 1992. Monoclonal antibodies against the native urease of *Helicobacter pylori*: synergistic inhibition of urease activity by monoclonal antibody combinations. Infect Immun **60:**4826–4831.
29. **Borlace GN, Jones HF, Keep SJ, Butler RN, Brooks DA.** 2011. *Helicobacter pylori* phagosome maturation in primary human macrophages. Gut Pathog **3:**3. http://dx.doi.org/10.1186/1757-4749-3-3.
30. **Ramarao N, Meyer TF.** 2001. *Helicobacter pylori* resists phagocytosis by macrophages: quantitative assessment by confocal microscopy and fluorescence-activated cell sorting. Infect Immun **69:**2604–2611. http://dx.doi.org/10.1128/IAI.69.4.2604-2611.2001.
31. **Green LC, Wagner DA, Glogowski J, Skipper PL, Wishnok JS, Tannenbaum SR.** 1982. Analysis of nitrate, nitrite, and [^{15}N]nitrate in biological fluids. Anal Biochem **126:**131–138. http://dx.doi.org/10.1016/0003-2697(82)90118-X.
32. **Faghri J, Poursina F, Moghim S, Zarkesh Esfahani H, Nasr Esfahani B, Fazeli H, Mirzaei N, Jamshidian A, Ghasemian Safaei H.** 2014. Morphological and bactericidal effects of different antibiotics on *Helicobacter pylori*. Jundishapur J Microbiol **7:**e8704.
33. **Graham DY, Malaty HM, Evans DG, Evans DJ, Jr, Klein PD, Adam E.** 1991. Epidemiology of *Helicobacter pylori* in an asymptomatic population in the United States. Effect of age, race, and socioeconomic status. Gastroenterology **100:**1495–1501.
34. **Mattsson A, Tinnert A, Hamlet A, Lonroth H, Bolin I, Svennerholm AM.** 1998. Specific antibodies in sera and gastric aspirates of symptomatic and asymptomatic *Helicobacter pylori*-infected subjects. Clin Diagn Lab Immunol **5:**288–293.
35. **Enroth H, Wreiber K, Rigo R, Risberg D, Uribe A, Engstrand L.** 1999. In vitro aging of *Helicobacter pylori*: changes in morphology, intracellular composition and surface properties. Helicobacter **4:**7–16. http://dx.doi.org/10.1046/j.1523-5378.1999.09034.x.
36. **Moran AP.** 2008. Relevance of fucosylation and Lewis antigen expression in the bacterial gastroduodenal pathogen *Helicobacter pylori*. Carbohydr Res **343:**1952–1965. http://dx.doi.org/10.1016/j.carres.2007.12.012.
37. **Hidaka E, Ota H, Hidaka H, Hayama M, Matsuzawa K, Akamatsu T, Nakayama J, Katsuyama T.** 2001. *Helicobacter pylori* and two ultrastructurally distinct layers of gastric mucous cell mucins in the surface mucous gel layer. Gut **49:**474–480. http://dx.doi.org/10.1136/gut.49.4.474.
38. **Xu Y, Jing JJ, Gong YH, Xu Q, Zhang WL, Piao Y, Wang YL, Yuan Y.** 2011. Changes in biological and virulent characteristics of *Helicobacter pylori* exposed to high salt. Asian Pac J Cancer Prev **12:**2637–2641.
39. **Barry DP, Asim M, Leiman DA, de Sablet T, Singh K, Casero RA, Jr, Chaturvedi R, Wilson KT.** 2011. Difluoromethylornithine is a novel inhibitor of *Helicobacter pylori* growth, CagA translocation, and interleukin-8 induction. PLoS One **6:**e17510. http://dx.doi.org/10.1371/journal.pone.0017510.
40. **Khamri W, Moran AP, Worku ML, Karim QN, Walker MM, Annuk H, Ferris JA, Appelmelk BJ, Eggleton P, Reid KB, Thursz MR.** 2005. Variations in *Helicobacter pylori* lipopolysaccharide to evade the innate immune component surfactant protein D. Infect Immun **73:**7677–7686. http://dx.doi.org/10.1128/IAI.73.11.7677-7686.2005.
41. **Zullo A, Hassan C, Ridola L, Repici A, Manta R, Andriani A.** 2014. Gastric MALT lymphoma: old and new insights. Ann Gastroenterol **27:**27–33.
42. **Wang X, Willen R, Svensson M, Ljungh A, Wadstrom T.** 2003. Two-year follow-up of *Helicobacter pylori* infection in C57BL/6 and Balb/cA mice. APMIS **111:**514–522. http://dx.doi.org/10.1034/j.1600-0463.2003.1110410.x.
43. **Wang X, Willen R, Andersson C, Wadstrom T.** 2000. Development of high-grade lymphoma in *Helicobacter pylori*-infected C57BL/6 mice. APMIS **108:**503–508. http://dx.doi.org/10.1034/j.1600-0463.2000.d01-89.x.
44. **Craig VJ, Cogliatti SB, Arnold I, Gerke C, Balandat JE, Wundisch T, Muller A.** 2010. B-cell receptor signaling and CD40 ligand-independent T cell help cooperate in *Helicobacter*-induced MALT lymphomagenesis. Leukemia **24:**1186–1196. http://dx.doi.org/10.1038/leu.2010.76.